Proceedings of the 21st ICSMGE, Vienna, Austria, 14 – 19 June 2026. Pistrol, Adam & Schweiger (eds.)
Published by: ÖGG, Austrian Society for Geomechanics, Salzburg, Austria, ISBN 978-3-9503898-4-5
https://doi.org/10.53243/ICSMGE2026-2331

Controlling moisture in historic sites with low water retention sand covers

Wei Wo, Mai Sawada
Department of Civil and Environmental Engineering, Institute of Science Tokyo, Tokyo, Japan, wo.w.a41a@m.isct.ac.jp

ABSTRACT: Severe soil moisture loss happens at historic sites due to evaporation during the archeological investigation excavation, which induces cohesion reduction, cracks, and mechanical instability. However, methods to mitigate the desiccation-induced damage are still under investigation. This study introduces a low-water retention sand cover and experimentally examines its impact on evaporation speed. Furthermore, moisture transfer during excavation in a burial mound was numerically simulated and the applicability of the sand cover protection was investigated. The results of the laboratory evaporation test under constant hydrothermal environment showed that an 8.5 mm-thick sand layer reduced the early-stage evaporation amount by 82%, compared to bare soil. The period of the early stage corresponds to the average natural rainfall interval, implying the possible practical application in situ. The numerical simulation showed that the excavation caused serious moisture loss locally in the burial mound above the stone chamber when the excavated surface was not covered with a sand cover, and a high water-content interlayer around the stone chamber was generated during the rainfall period. These negative effects were mitigated when the excavated surface was covered with a 10mm-thick protective sand cover. The sand cover reduced evaporation and made soil the moisture distribution uniform, creating the horizontal water transfer to the desiccation area without water supply. This work demonstrated that sand cover protection is useful to mitigate moisture variation in historic sites during excavation and contributes to better preservation.

KEYWORDS: Unsaturated soil, evaporation, water retention.

1 INTRODUCTION

Archeological excavation removes buried soil from historic sites and exposes the remains to drastic environmental changes. Rainfall infiltration and evaporation desiccation raise the risk of soil mechanical stability loss and physicochemical degradation of burial goods, while the studies in geotechnical preservation methods are insufficient. Moisture control methods are necessary for better preservation of archeological sites.

The Tsugeyama tumulus is a precious ancient soil heritage, located in Takatsuki City, Osaka, Japan. The tumulus was registered as Japan historic site in 2002, when several valuable burial goods were found in its 2 stone chambers free from tomb robbery. The site geometry determined by a pre-excavation is shown in Figure 1 (Takatsuki City Buried Cultural Property Research Center, 2009). The burial goods should be removed from the stone chambers to preserve them in good condition under an optimum hydrothermal environment; however, excavation can accelerate soil moisture loss due to evaporation and may lead to an unsuitable environment, which finally can cause irreversible damage on the burial goods in a rather short time.

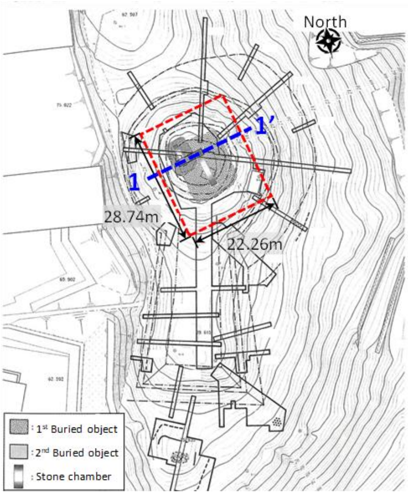

Figure 1. Location of the Tsugeyama tumulus mound and cross-section position. (Takatsuki City Buried Cultural Property Research Center, 2009)

This study introduces a protective sand cover to reduce evaporation and examines its applicability to the archeological site excavation. A laboratory evaporation test is performed to investigate the impacts of the sand cover on evaporation behavior. Furthermore, moisture transfer in the Tsugeyama tumulus during the excavation is numerically simulated at cross-section 1-1' in Figure 1, then the effectiveness of sand cover protection is also examined.

2 LABORATORY EVAPORATION TEST

2.1 *Materials and methods*

Evaporation reduces the moisture at the soil surface, requiring a vertical water transfer driven by suction gradient. However, sand easily loses moisture when exposed to the atmosphere due to its low water retention. This property rapidly causes an invasion of air into the soil, which blocks the water transfer path as shown in Figure 2, and finally results in a weak hydraulic conductivity. By reducing hydraulic conductivity at the surface, sand cover restrains the water supply speed to the soil surface, and mitigates evaporation.

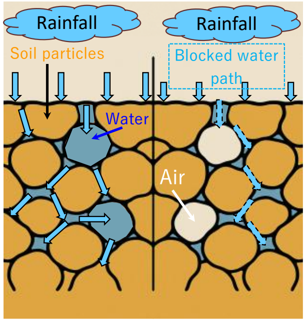

Figure 2. Mechanism of evaporation mitigation by sand

A laboratory elemental evaporation test was conducted to confirm the potential of sand cover, as shown in Figure 3(a). Decomposed granite soil with 40% fine fraction content was compacted in two acrylic boxes (150 mm × 150 mm × 50 mm). The gravimetric water content was 29% (degree of saturation was 82.6%) and the void ratio was 0.927. One specimen was covered by a Toyoura sand layer with a thickness of 8.5 mm, and the other was directly exposed to the atmosphere as a control case. The two specimens were placed in a constant environment chamber, setting at 20°C and 60%RH for 14 days. The specimen mass was measured with an electronic balance system every 15 min and the cumulative evaporation amount and speed were calculated correspondingly.

2.2 *Experiment results*

Figure 3(a) shows the moisture distribution after the tests. Although both specimens suffered evaporation, the sand cover slowed moisture loss. The ultimate gravimetric water content was 16.7% with the sand-covered specimen, while 4.0% in the bare case. Soil moisture slightly increased from the top surface to the bottom in both cases, while the deviation was larger as desiccation developed. The sand layer remained dry after the test, thus all the moisture loss was consumed by evaporation.

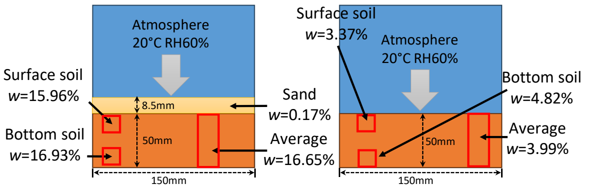

(a) Water content distribution of two boxes.

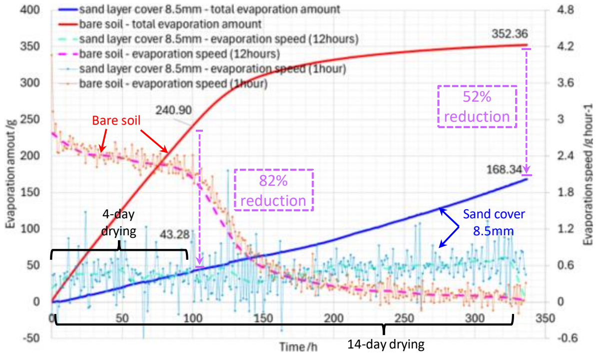

(b) Cumulative evaporation amount and speed graph of two boxes.

Figure 3. Laboratory elemental evaporation test result.

Figure 3(b) shows a time-series graph illustrating evaporation amount results on the left axis and speed results on the right axis. Both the average speed per 1 and 12 hours were plotted. The sand cover suppressed the evaporation speed at a relevant low but constant stage until the test end, as shown in blue curves; however, the bare soil exhibited a typical 3-stage evaporation speed pattern as red curves.

The difference in the total evaporation amount of the two specimens was 52% at the test end. Furthermore, the sand cover restricted the evaporation behavior by 82% during the first 4 days, which is the typical summer precipitation interval at the target site in Osaka, due to the huge evaporation speed gap at the beginning. This laboratory evaporation test highlights the feasibility and potential of sand cover, especially at the early evaporation stage (0~96h).

3 NUMERICAL SIMULATION

3.1 *Simulation methods*

Figure 4 shows a numerical model based on the 1-1' cross-section geometry (highlighted in Figure 1) of the Tsugeyama Tumulus. The soil layers are colored based on the future 4-stage excavation plan. The target tumulus is on the top of a hill with an elevation of approximately 80 m, therefore, an impermeable boundary was used, as underground behavior was not involved. This study focuses on the influence of the excavation on the 2nd (upper) stone chamber.

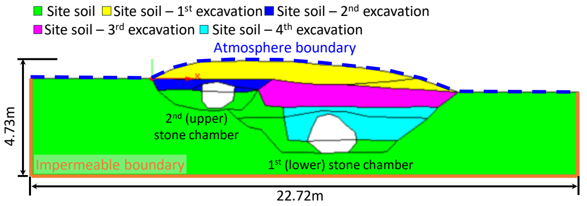

(a) Numerical model before excavation at 144h.

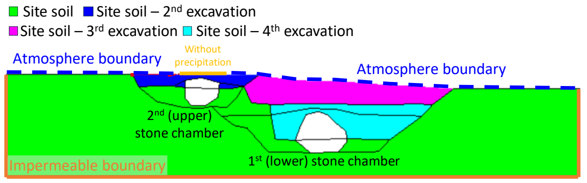

(b) Numerical model after 1st excavation at 144h.

Figure 4. Numerical model and excavation plan.

The total simulation duration was 288 h, where 4 wetting/drying loops were included (Figure 5). The excavation happened at 144 h. Two cases (with 0 mm and 10 mm sand cover) were simulated, and a special boundary condition was applied to the area above 2nd (upper) stone chamber in both cases, as shown in Figure 4 and 5. This boundary represents shelters for the excavated stone chamber from infiltration.

According to the local climate record of Osaka in August 2024, the average atmosphere condition 30°C/RH 60% were adopted in simulation. During wetting periods, The average rainfall intensity was 3.68mm/h.

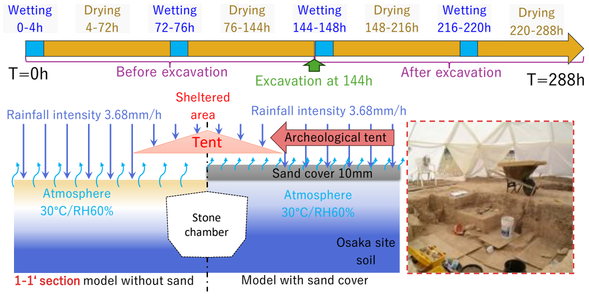

Figure 5. Simulation period and boundary condition.

Table 1. Material properties.

Properties	Site soil property	Sand property
Soil name	Tsugeyama site soil sample	Toyoura sand
Natural dry density	1.28 g/cm^3	1.55 g/cm^3
Soil particle density	2.72 g/cm^3	2.64 g/cm^3
Initial degree of saturation (*Sr*)	49.5%	≤1%
Saturated hydraulic conductivity	1.41×1e-5 m/s	2.084×1e-4 m/s
SWCC – α	0.890 kPa^{-1}	0.317 kPa^{-1}
SWCC – *n*	1.188	7.38
SWCC – θ_s	0.53	0.413
SWCC – θ_r	0	0

Van Genuchten model (1980) was used in SWCC fitting

The numerical simulation was performed by Code_Bright, a FEM program for thermo-hydro-mechanical analysis (UPC Department of Civil and Environmental Engineering, n.d.). The soil properties obtained from laboratory tests are listed in Table 1.

3.2 *Simulation results and discussions*

Figure 6 shows the degree of saturation (*Sr*) deviation at 144 h after 2 wetting/drying loops before the excavation. The area around 2nd (upper) chamber is focused and zoomed in. Based on the distribution, the stone chamber was in a stable environment under the protection of burial soil. The wetting/drying loops only influence the shallow zone. Therefore, protective actions are not necessary before the excavation.

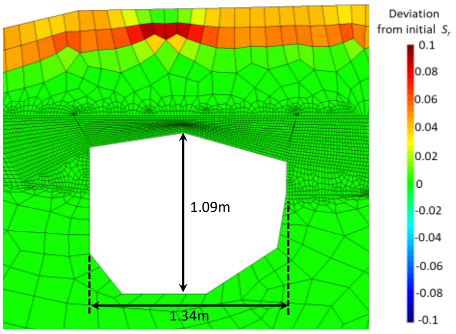

Figure 6. *Sr* deviation around stone chamber before excavation.

However, once the soil is excavated, the stone chamber would be placed in a different condition. Figure 7 is the degree of saturation (*Sr*) distribution around the stone chamber at 288 h for both bare soil and sand-covered soil. This timing corresponds to extra wetting/drying loops after excavation.

A severe desiccation was found at the sheltered area (Figure 7(a)). *Sr* reduced from 49.5% to around 20%, shown in the blue painted area. This indicates that rapid moisture loss happens after excavation. The area which was not sheltered by the tent was wetter, as rainfall compensated for evaporation. *Sr* of the unsheltered area reached 40%, which is very close to the initial *Sr* (49.5%). This fact reflects the natural water content equilibrium at the site under in situ climate conditions.

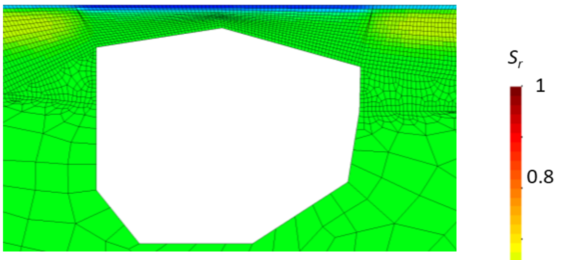

(a) Bare soil case, *Sr* distribution around chamber.

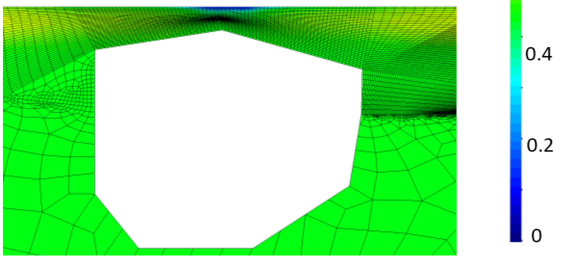

(b) Sand cover case, *Sr* distribution around chamber.
Figure 7. *Sr* distribution comparation between two cases.

As for vertical *Sr* distribution, the desiccation area above the chamber extended to a depth of 5 cm, as shown in Figure 7(a). This is consistent with the previous laboratory test results. A high water-content interlayer was observed at a depth of about 10 cm in the unsheltered area. This interlayer was generated by the small hydraulic conductivity at the shallow layer when *Sr* was low. The air invasion in the soil reduced hydraulic conductivity by blocking the water transfer path. A rapid downward rainwater seepage occurred; however, as the soil surface moisture reduced, the upward water transfer was restricted due to the low hydraulic conductivity, although the suction gradient was large and thus, a high water-content interlayer remained between the surface and deep zone.

The sand cover impacted the soil moisture distribution (Figure 7(b)). The overall soil status was in a wetter condition, compared to the bare soil case. Although *Sr* of the soil above the chamber decreased to 20%, the severe desiccation area significantly decreased by the sand cover as it mitigated the evaporation in the sheltered zone. The area without the shelter showed a similar behavior to the bare soil case, and *Sr* was around 60%. It should be noted that the sand cover did not increase *Sr* during wetting. The maximum *Sr* was around 75% in both cases. This means the soil water retention was improved by the sand cover, without causing negative effects.

As for the vertical *Sr* distribution, the desiccation zone above the chamber shrank in both horizontal and vertical direction, while the high water-content interlayer at the unsheltered zone disappeared. The higher hydraulic conductivity and faster water transfer under the sand cover allowed the moisture redistribution in the vertical direction after rainfall, and thus, the interlayer was not formed. Another notable point is the moisture redistribution in the horizontal direction toward the sheltered area due to a relatively high water-content zone above the chamber.

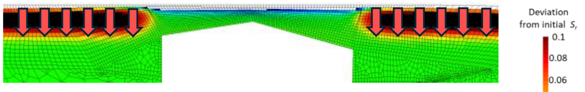

(a) Bare soil case, *Sr* deviation and water flow.

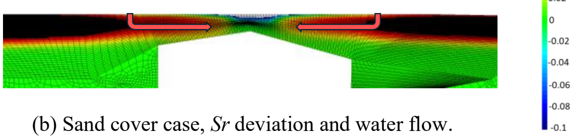

(b) Sand cover case, *Sr* deviation and water flow.
Figure 8. *Sr* deviation and water flow pattern of two cases.

Figure 8 compares the *Sr* deviations from the initial status between the bare soil and sand-covered cases. The wetter soil (more than 10% increase) was painted black, while the dryer soil (more than 10% decrease) was painted in white. The water flow was highlighted with arrows.

According to Figure 8(a), a large desiccation area was found above the stone chamber. Besides that, the unsheltered area experienced desiccation in the shallow zone. The high water-content interlayer with vertical seepage flow was observed, while the seepage flow was strictly limited within the unsheltered zone, as the horizontal water path was blocked by desiccation zone.

In the sand-cover case (Figure 8(b)), the desiccation zone above the chamber, represented by the white painted parts, was small compared to the bare soil case. In the unsheltered zone, the shallow zone was wetter than the initial status (painted in black). The interlayer at the unsheltered zone was replaced by a large continuous high water-content part, indicating the occurrence of water redistribution. The most attractive phenomenon was the high moisture zone above the stone chamber.

Since the sheltered area could not receive a direct water supply, the only source of moisture must be the horizontal water transfer from the unsheltered area. The sand cover kept moisture with a higher hydraulic conductivity, and the water path allowed horizontal water transfer with a small suction gradient. The horizontal indirect water supply resulted in high *Sr*, which promoted the following water transfer.

These results show that the sand cover is useful for controlling moisture in archeological sites by not only directly mitigating evaporation, but also by indirectly supplying water.

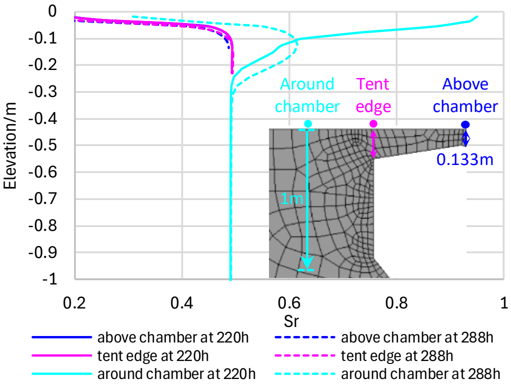

(a) Bare soil case, *Sr* vertical profile at different stage.

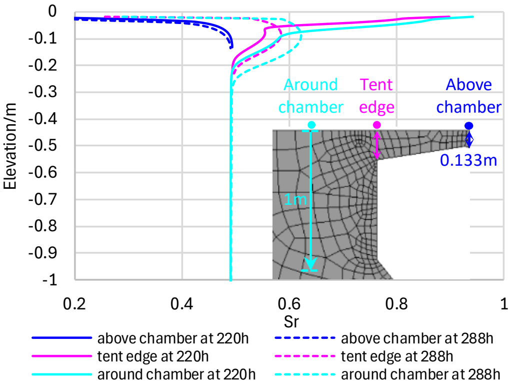

(b) Sand cover case, *Sr* vertical profile at different stage.

Figure 9. Sand cover effects on three different positions.

Figure 9 plots the *Sr* vertical profiles at three different positions: "above chamber", "tent edge", and "around chamber". The curve colors represent these positions, and the solid and dashed lines represent the results at 220 h (immediately after rainfall) and 288 h (after the evaporation process), respectively.

Figure 9(a) shows the results of the bare soil case. The blue curves (above chamber) are invisible due to the overlapping with the pink curves (tent area) for both solid and dashed lines. This indicates that the moisture distribution was uniform in the horizontal direction between the tent edge and center, and evaporation predominantly affected the moisture transfer.

As for the position around the chamber, an obvious *Sr* variation was observed, especially after rainfall (220 h). The soil surface was nearly fully saturated, while the rainfall impacted up to a depth of 30 cm. This proves the necessity of the tent, since the upper soil thickness above the stone chamber was not sufficient to protect the chamber from infiltration and evaporation. At 288 h, the shallow zone at a depth less than 10 cm was dry, while the deeper zone (10-30 cm) was wet compared to the previous time section.

Figure 9(b) represents the results of the sand-covered case. The soil above the chamber was dry, and the solid and dashed lines were very close to each other, indicating slow evaporation after the most active 1st stage. The results at the tent edge were very similar to those around the chamber, although they were under completely different boundary conditions. With the horizontal water supply from the surrounding soil, the *Sr* variations at these two points were synchronized, since both exhibited an increase of *Sr* at 0-10 cm soil layer after rainfall at 220 h and at 10-30 cm soil layer after evaporation. These results show the existence of both horizontal and vertical water transfers that mitigate moisture variation.

4 CONCLUSION

1. The laboratory tests demonstrated that sand covers greatly reduced the evaporation amount, particularly, in the most active evaporation stage 1, which resulted in an up to 82% evaporation reduction in a typical 3-day's precipitation interval, and 52% reduction in 14-day's drying period.
2. The simulation results showed that it is necessary to take protective actions during excavation to avoid a serious soil moisture loss above the target chamber that can induce damage within a very short term.
3. The sand cover mitigated evaporation by two mechanisms: (a) directly improved the soil water retention ability, and (b) kept the water transfer paths for moisture redistribution and water supply from the surrounding area. The sand cover provides a suitable and moderate environment variation for the stone chamber.

5 ACKNOWLEDGEMENTS

The authors appreciate the Cultural Affairs Division of Takatsuki City providing us with the burial mound soil for laboratory tests. This work was supported by JST SPRING, Japan Grant Number JPMJSP2106 and JPMJSP2180.

6 REFERENCES

Takatsuki City Buried Cultural Property Research Center (ed.), 2009. *Investigative report on the Tsugeyama Kofun historic site*. Takatsuki City Board of Education. (In Japanese)

UPC Department of Civil and Environmental Engineering, n.d. *CODE_BRIGHT: A Finite Element Program for Thermo-Hydro-Mechanical Analysis in Geological Media*. [online] Universitat Politècnica de Catalunya. Available at: https://deca.upc.edu/en/projects/code_bright [Accessed 7th June 2025].

Van Genuchten, M.Th., 1980. A closed-form equation for predicting the hydraulic conductivity of unsaturated soils. *Soil Science Society of America Journal*, 44(5), 892–898.